

## Influence of copper content on structural features and performance of pre-reduced $\text{LaMn}_{1-x}\text{Cu}_x\text{O}_3$ ( $0 \leq x < 1$ ) catalysts for methanol synthesis from $\text{CO}_2/\text{H}_2$

JIA Lishan (贾立山)<sup>1,2</sup>, GAO Jing (高敬)<sup>1,2</sup>, FANG Weiping (方维平)<sup>3</sup>, LI Qingbiao (李清彪)<sup>1,2</sup>

(1. Department of Chemical Engineering and Biochemical Engineering, College of Chemistry and Chemical Engineering, Xiamen University, Xiamen 361005, China; 2. National Engineering Laboratory for Green Chemical Productions of Alcohols, Ethers and Esters, Xiamen 361005, China; 3. Department of Chemistry, College of Chemistry and Chemical Engineering, Xiamen University, Xiamen 361005, China)

Received 13 April 2010; revised 14 May 2010

**Abstract:** A series of pre-reduced  $\text{LaMn}_{1-x}\text{Cu}_x\text{O}_3$  ( $0 \leq x < 1$ ) catalysts for methanol synthesis from  $\text{CO}_2$  hydrogenation were prepared by a sol-gel method. The catalytic performances were strongly dependent on the copper content. XRD investigation revealed that the single perovskite structure could be preserved after being reduced, when the substitution for Mn by Cu was less than 50%. The Cu-doped ( $x=0.5$ )  $\text{LaMnO}_3$  was much more active than the other catalysts for reaction, showing  $\text{CO}_2$  conversion up to 11.33% and methanol selectivity close to 82.14%. The structural features of samples ( $x \leq 0.5$ ) were studied. It was determined that copper existed as  $\text{Cu}^+$  species under reduction conditions.  $\text{H}_2$  was adsorbed on  $\text{Cu}^+$  sites and  $\text{CO}_2$  was activated on the medium  $\text{CO}_2$  active species in the lattice. The strong interaction between  $\text{Cu}^+$  and Mn inhibited the further reduction from  $\text{Cu}^+$  to  $\text{Cu}^0$  and made the fine dispersion of medium basic site to adsorb  $\text{CO}_2$ , contributing to reactivity.

**Keywords:**  $\text{LaMn}_{1-x}\text{Cu}_x\text{O}_3$  perovskite; sol-gel method;  $\text{CO}_2$  hydrogenation; methanol; rare earths

It is well known that carbon dioxide emissions have induced global warming. The technologies of exploitation and fixation of  $\text{CO}_2$  as the major strategies have received much attention at present. Indeed, catalytic hydrogenation of carbon dioxide to methanol is one of the attractive approaches, since methanol is a key material for many chemicals, as well as an alternative energy substitute for the oil-based fuels of automobiles<sup>[1]</sup>.

Considerable research efforts have been directed to development of catalysts which show high activity towards methanol synthesis from carbon dioxide hydrogenation<sup>[2-6]</sup>.  $\text{AB}_{1-x}\text{B}'_x\text{O}_3$  (A and B (B') are usually a lanthanide and transition metal, respectively, and  $x$  is the substitution degree) perovskite-type oxides have been reported to catalyze many reactions after being reduced under proper conditions. Activity is governed by nature of the cation in position B and related to reducibility. Meanwhile, the partial substitution of B-sites gives rise to a modification in catalytic behavior for some reactions. Compared with conventional preparation methods, this method could lead to a fine particle size and a high dispersion of active sites. For example, Navarro et al.<sup>[7]</sup> added Ru to  $\text{LaCoO}_3$ , which increased activity and stability of  $\text{LaCoO}_3$ -derived catalyst for hydrogen production by oxidative reforming of diesel. Araujo et al.<sup>[8]</sup> also pointed out that  $\text{LaNi}_{1-x}\text{Ru}_x\text{O}_3$  was active in methane reforming with  $\text{CO}_2$  and was not accompanied by coke deposition. Tien-Thao et al.<sup>[9]</sup> found that  $\text{LaCo}_{1-x}\text{Cu}_x\text{O}_{3-\delta}$  catalysts featured higher-alcohol in CO hydrogenation. The addition of copper into  $\text{LaCoO}_3$  framework led to changes in product

distribution of reaction. Petrović et al.<sup>[10]</sup> studied the Pd-doped perovskite phase  $\text{LaTi}_{0.5}\text{Mg}_{0.5}\text{O}_3$  catalysts. They found that Pd content in the mixed perovskite had a little influence on activity of methane oxidation over high temperature, connected with particle size effects and metal-perovskite interactions.

Previously, we have shown that carbon dioxide hydrogenation to methanol over the pre-reduced  $\text{LaCr}_{0.5}\text{Cu}_{0.5}\text{O}_3$  catalyst. It was found that the reduced Cu-based  $\text{LaCr}_{0.5}\text{Cu}_{0.5}\text{O}_3$  catalyst displayed high catalytic performance in comparison with 13% Cu/ $\text{LaCrO}_3$ . Copper is assumed as an active metal for the formation of alcohols (mainly methanol) but manganese is not a typical catalyst for propagation of hydrocarbon chain of products<sup>[11]</sup>. The chemical stability of  $\text{LaMnO}_3$  perovskite phase is higher than that of  $\text{LaCrO}_3$ , due to its lower electronegativity<sup>[12]</sup>. This leads to the assumption that a combination of Mn and Cu element in the desired perovskite structure could be a promising catalyst precursor for the synthesis of methanol from  $\text{CO}_2/\text{H}_2$ . At present, the substitution of Mn by Cu in  $\text{LaMnO}_3$  has been reported to catalyze the reactions of oxygenate synthesis from syngas and reduction of NO by CO or propene. Partial Cu substitution can enhance the abundance of anion vacancies and the mobility of lattice oxygen in lanthanites, contributing to a significant improvement in catalytic performance<sup>[11,13,14]</sup>. The present work was to investigate the effect of copper content on structural features and catalytic behavior for  $\text{CO}_2$  hydrogenation to methanol over the pre-reduced  $\text{LaMn}_{1-x}\text{Cu}_x\text{O}_3$  catalysts ( $0 \leq x < 1$ ). The structural properties of

catalysts were characterized by X-ray diffraction (XRD), X-ray electron spectroscopy (XPS), temperature programmed desorption ( $H_2/CO_2$ -TPD) and Raman measurements.

## 1 Experimental

### 1.1 Catalyst preparation

$LaMn_{1-x}Cu_xO_3$  oxides with  $0 \leq x < 1$ , were prepared by a sol-gel method using citric acid as a complexing agent. The amounts of precursor salts ( $La(NO_3)_3 \cdot nH_2O$  ( $La_2O_3 \geq 44\%$ ),  $Mn(NO_3)_2$ ,  $Cu(NO_3)_2 \cdot 3H_2O$ ) along with citric acid were dissolved in water at a molar ratio of 2:1 (metal cations: citric acid). The total metal cation concentration was fixed to be 0.2 mol/L. The solution was heated to 150 °C until it was ignited. The resulting powder was finally calcined in air at 400 °C for 2 h and then at 800 °C for 4 h.

### 1.2 Catalyst reaction

The methanol synthesis reaction was carried out in a fixed-bed flow reactor. Prior to the reaction, the precursor of catalyst (0.5 g) was pre-reduced with pure  $H_2$  at 350 °C for 2 h under atmospheric pressure. Then the reactor was cooled to 200 °C and the reaction gas was admitted at the pressure of 2 MPa. The reaction of  $CO_2$  hydrogenation was tested at 250 °C. A  $CO_2$ - $H_2$  reaction mixture in the molar ratio equal to 1:3 was fed at a space velocity (GHSV) of 2400 ml/(h·g). The products were analyzed by an on-line gas chromatograph (GC-950) using TDX-01 column and GDX-401 column, connected to TCD and FID, respectively. The former column was used for the separation of  $N_2$ , CO and  $CO_2$ , while the latter was used for the separation of methane and methanol. Conversion and selectivity values were calculated by the internal standard and mass-balance methods.

### 1.3 Characterization

Powder X-ray diffraction (XRD) patterns were recorded on a Panalytical X'Pert Pro X-ray diffractometer with Cu  $K\alpha$  radiation, in the step mode ( $0.0167^\circ$ , 15 s) in the range  $20^\circ < 2\theta < 80^\circ$ . The voltage and current were 40 kV and 30 mA, respectively.

X-ray photoelectron spectroscopy (XPS) measurements were done on a Quantum 2000 Scanning ESCA microprobe instrument with Al  $K\alpha$  radiation (15 kV, 150 W,  $h\nu=1486.6$  eV) under ultrahigh vacuum ( $10^{-7}$  Pa), calibrated internally by the carbon deposit C(1s) ( $E_b=284.8$  eV).

$H_2$ -temperature-programmed desorption ( $H_2$ -TPD) was conducted on Micromeritics AutoChem 2920 II instrument connected to a ThermoStar GSD 301 T2 mass spectrometer. About 100 mg of the catalyst sample was used for each test. The precursor of catalyst was firstly pre-reduced *in situ* in the TPD equipment by pure  $H_2$  at 350 °C for 2 h, followed by switching to a  $H_2$  (99.999%, purity) stream for adsorption at 45 °C for 1 h. The  $H_2$  desorption was then performed from 50 to 700 °C at a rate of 10 °C/min.  $CO_2$ -TPD was carried

out under the same condition as  $H_2$ -TPD, conducting from 50 to 450 °C.

Confocal Raman microspectroscopy was conducted at room temperature with Renishaw UV-Vis Raman 1000 System, equipped with a CCD (charge couple device) detector and a Leica DMLM microscope. The line at 514.5 nm of an  $Ar^+$  laser was used for excitation. The laser power was reduced to  $\sim 1.0$  mW for ensuring that no sample damage was caused by the laser irradiation.

## 2 Results and discussion

### 2.1 XRD analysis

Fig. 1 depicts the main characteristics of fresh (a) and reduced (b)  $LaMn_{1-x}Cu_xO_3$  perovskites ( $0 \leq x < 1$ ). For the fresh  $LaMn_{1-x}Cu_xO_3$  series ( $x \leq 0.5$ ), as shown in Fig. 1(a), the only phase was a single perovskite phase (JCPDS 01-075-0440), indicating the substitution of Cu in Mn site when Cu content was less than 0.5<sup>[15]</sup>. The phase composition was changed in the used catalyst with  $x=0.7$ , the oxygen vacancies were so high that  $La_2CuO_4$  phase appeared, besides a remaining Mn-Cu perovskite phase. Meanwhile, copper oxide phase characterized by two strong reflections at  $2\theta=35.62^\circ$  and  $38.76^\circ$  were clearly observed with the substitution for Mn by 90% Cu, implying that a noticeable number of copper ions was still located out of the perovskite lattice. This result accorded with the literature findings reported by Porta et al.<sup>[16]</sup>.

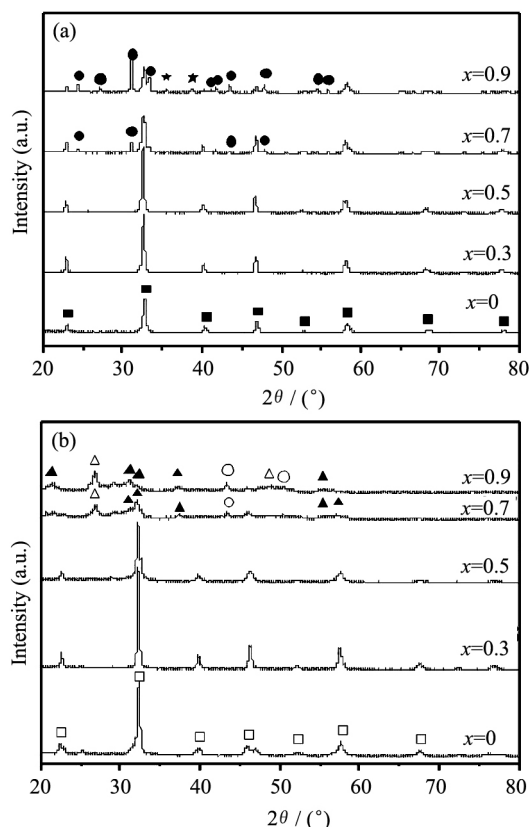


Fig. 1 XRD patterns of the fresh (a) and reduced (b)  $LaMn_{1-x}Cu_xO_3$  (■)  $LaMnO_3$ ; (●)  $La_2CuO_4$ ; (★) CuO; (□)  $La_{1-x}Mn_{1-x}O_3$ ; (▲)  $LaMnO_3$ ; (△)  $La_2O_3$ ; (○) Cu

Moreover, the substitution of Mn with Cu in perovskites has led to a decline in the diffraction lines. It was attributed to the difference between ionic radii of  $\text{Cu}^{2+}$  (0.0730 nm) and  $\text{Mn}^{3+}$  (0.0645 nm), leading to a little change in unit cell of perovskite lattice<sup>[17]</sup>. The main diffraction peak at  $2\theta=32.80^\circ$  with  $x=0$  shifted to the lower angle  $2\theta=32.63^\circ$  and  $32.58^\circ$  with  $x=0.3$  and  $x=0.5$ , respectively. XRD patterns were also obtained for catalysts reduced at 350 °C, as shown in Fig. 1(b). The only reduction product was also a perovskite-like single phase  $\text{La}_{1-x}\text{Mn}_{1-z}\text{O}_3$  (JCPDS 00-051-1516) when  $x \leq 0.5$ . The main diffraction line at  $2\theta$  shifted to the much lower angle  $32.32^\circ$ ,  $32.26^\circ$  and  $32.15^\circ$  with  $x=0$ ,  $x=0.3$ , and  $x=0.5$ , respectively. And along with the increase of Cu doping, the intensity of diffraction peaks of  $\text{La}_{1-x}\text{Mn}_{1-z}\text{O}_3$  weakened gradually, while the line width broadened slightly. The XRD patterns of the reduced catalysts showed some weak reflection lines of  $\text{LaMnO}_3$  (JCPDS 01-085-2219),  $\text{La}_2\text{O}_3$  (JCPDS 01-089-4016) and Cu (JCPDS 01-089-2838) phases, when the substitution for Mn by Cu was prepared up to 90%.

### 2.2 Reaction activity

The catalytic performances of catalysts for  $\text{CO}_2$  hydrogenation to methanol are summarized in Table 1. The major product was methanol, and the by-products were CO and methane, of which CO was the major one due to “reverse-water-gas-shift (RWGS) reaction”. It was found that the substitution of Mn by Cu in the perovskite had an influence on the catalytic behavior that the selectivity of  $\text{CH}_3\text{OH}$  and the conversion of  $\text{CO}_2$  were improved significantly. Firstly, the catalytic activity of Cu-doped  $\text{LaMnO}_3$  was much higher than that of undoped  $\text{LaMnO}_3$  for hydrogenation of carbon dioxide, especially to produce methanol. Secondly, the yield of methanol did not always increase with the increasing substituted Cu-containing and it was up to the highest value when  $x=0.5$ , with the  $\text{CO}_2$  conversion of 11.33% and methanol selectivity of 82.14%. Lastly, the selectivity of methanol over catalysts with  $x \leq 0.5$  was much higher than that over catalysts with  $x > 0.5$ . Therefore, the characterizations of  $\text{LaMn}_{1-x}\text{Cu}_x\text{O}_3$  ( $x \leq 0.5$ ) would be further studied as follows, in view of the complexity of phases when  $x=0.7$  and  $0.9$ .

### 2.3 XPS investigations

XPS spectra of  $\text{LaMn}_{1-x}\text{Cu}_x\text{O}_3$  ( $x=0.3$  and  $0.5$ ) before and after being reduced are presented in Fig. 2 (a) and (b), providing direct experimental evidence about valence states of Cu species.  $\text{Cu}^{2+}$  had the BE of  $\text{Cu } 2p_{3/2}$  band above 933.5 eV

**Table 1 Performance of catalysts for  $\text{CO}_2$  hydrogenation\***

$\text{LaMn}_{1-x}\text{Cu}_x\text{O}_3$	$X_{\text{CO}_2}/\%$	$S_{\text{MeOH}}/\%$	$S_{\text{CO}}/\%$	$S_{\text{CH}_4}/\%$
$x=0.9$	1.28	9.32	46.12	44.56
$x=0.7$	3.79	36.17	36.34	27.49
$x=0.5$	11.33	82.14	13.83	4.03
$x=0.3$	3.94	68.1	26.38	5.52
$x=0$	0.83	0	55.83	44.17

\* Reaction conditions:  $P=2$  MPa, GHSV=2400 ml/(h·g),  $\text{CO}_2:\text{H}_2=1:3$  (molar ratio)

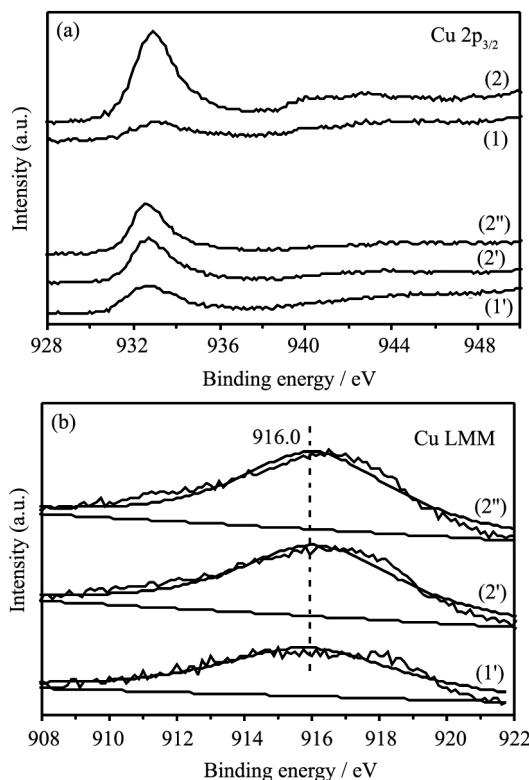


Fig. 2 XPS-Auger spectra of Cu  $2p_{3/2}$  (a) and Cu LMM (b) (1) the fresh  $\text{LaMn}_{0.7}\text{Cu}_{0.3}\text{O}_3$ ; (2) the fresh  $\text{LaMn}_{0.5}\text{Cu}_{0.5}\text{O}_3$ ; (1') the reduced  $\text{LaMn}_{0.7}\text{Cu}_{0.3}\text{O}_3$  for 2 h; (2') the reduced  $\text{LaMn}_{0.5}\text{Cu}_{0.5}\text{O}_3$  for 2 h; (2'') the reduced  $\text{LaMn}_{0.5}\text{Cu}_{0.5}\text{O}_3$  for 11 h

with a shake-up peak and it was absent on the reduced surface. Since the BE of Cu  $2p_{3/2}$  bands in  $\text{Cu}^0$  (932.67 eV) and in  $\text{Cu}^+$  (932.4 eV) are almost the same, they can be distinguished by different kinetic energy of the Cu LMM line position in metal (918.65 eV) and  $\text{Cu}_2\text{O}$  (916.8 eV)<sup>[18]</sup>. The result indicated that the chemical state of copper existed as  $\text{Cu}^+$  species after the Cu-doped  $\text{LaMnO}_3$  being reduced for both 2 and 11 h. That was why there was no  $\text{Cu}^0$  peak in XRD patterns of the reduced catalysts. In numerous studies, it has been confirmed that the stabilization of the  $\text{Cu}^+$  ions on the support favors the hydrogenation of  $\text{CO}_2$ <sup>[19]</sup>. The  $\text{Cu}^+$  ions could also be stabilized on the surface of perovskite. According to Fujita et al.<sup>[20]</sup> the presence of  $\text{Cu}^+$  accelerated the reduction of  $\text{CO}_2$  to CO (RWGS) besides methanol, which would explain why the  $\text{LaMn}_{0.5}\text{Cu}_{0.5}\text{O}_3$  catalyst was less selective towards methanol, compared with the  $\text{LaCr}_{0.5}\text{Cu}_{0.5}\text{O}_3$  catalyst, as reported in the case of  $\text{LaCr}_{1-x}\text{Cu}_x\text{O}_3$ <sup>[21]</sup>.

### 2.4 $\text{CO}_2$ -TPD

Fig. 3 depicts  $\text{CO}_2$ -TPD profiles of the reduced  $\text{LaMn}_{1-x}\text{Cu}_x\text{O}_3$  ( $x=0, 0.3$  and  $0.5$ ) and the fresh  $\text{LaCr}_{0.5}\text{Cu}_{0.5}\text{O}_3$ , detecting concentration of surface basic sites and basic strength. The first main TPD peak around 100 °C appeared for all the samples, originating from weak  $\text{CO}_2$  adsorption. The subsequent peak was found in the range from 250 to 350 °C, corresponding to medium basic sites<sup>[22]</sup>. It was also observed that the second desorption peak shifted to the high temperature with the increasing copper content. The TPD

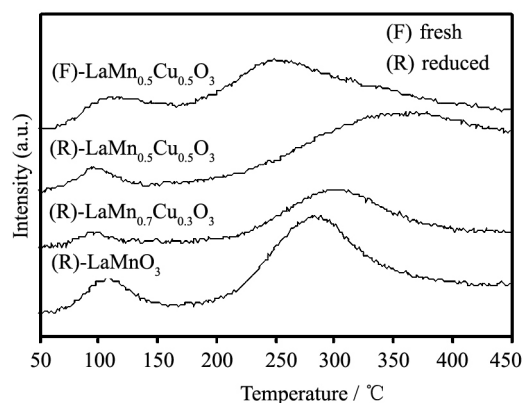


Fig. 3 CO<sub>2</sub>-TPD profiles of the reduced LaMn<sub>1-x</sub>Cu<sub>x</sub>O<sub>3</sub> ( $x=0, 0.3$  and  $0.5$ ) and the fresh LaMn<sub>0.5</sub>Cu<sub>0.5</sub>O<sub>3</sub>

profiles of the fresh LaMn<sub>0.5</sub>Cu<sub>0.5</sub>O<sub>3</sub> showed a desorption peak around 250 °C, lower than those of the reduced LaMn<sub>1-x</sub>Cu<sub>x</sub>O<sub>3</sub>. This result disclosed an interaction between Cu<sup>+</sup> and Mn. And the interaction increased with the Cu content. It was found that the area of medium CO<sub>2</sub> desorption peak for  $x=0.5$  was larger than those for  $x=0$  and  $0.3$ . As the medium CO<sub>2</sub> active species can be better dispersed on the surface of catalyst over  $x=0.5$ , the better the dispersion, the more the adsorption of CO<sub>2</sub>.

## 2.5 Raman data

Fig. 4 shows Raman spectra of LaMn<sub>1-x</sub>Cu<sub>x</sub>O<sub>3</sub> ( $x=0, 0.3$  and  $0.5$ ) compounds after being reduced, measured at room temperature, which displays peaks located around 530 and 660 cm<sup>-1</sup>. According to lattice dynamic calculations, the peaks at 530 and 660 cm<sup>-1</sup> are associated with bending- and stretching-like vibrations of the Mn(Cu)O<sub>6</sub> octahedra, respectively<sup>[23]</sup>. It is noted that the intensity of Raman spectra over LaMn<sub>0.5</sub>Cu<sub>0.5</sub>O<sub>3</sub> was much higher than that over LaMn<sub>0.7</sub>Cu<sub>0.3</sub>O<sub>3</sub>. This result might be due to the stronger interaction between Mn/Cu ions over LaMn<sub>0.5</sub>Cu<sub>0.5</sub>O<sub>3</sub> than that over LaMn<sub>0.7</sub>Cu<sub>0.3</sub>O<sub>3</sub>, as Minh et al.<sup>[24]</sup> observed over LaMn<sub>1-x</sub>Ni<sub>x</sub>O<sub>3</sub>, which was in agreement with conclusion of CO<sub>2</sub>-TPD data. This interaction may be responsible for the harder Cu reduction process (Cu<sup>+</sup>→Cu<sup>0</sup>).

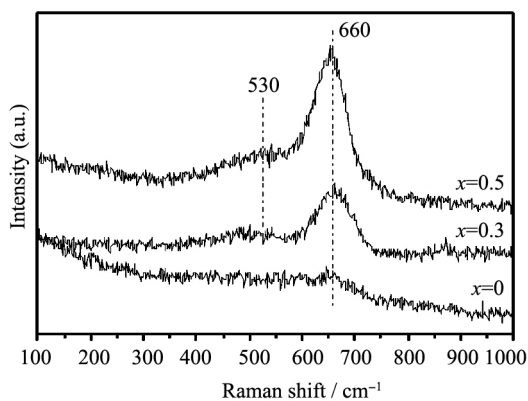


Fig. 4 Raman spectra of the reduced LaMn<sub>1-x</sub>Cu<sub>x</sub>O<sub>3</sub> ( $x=0, 0.3$  and  $0.5$ )

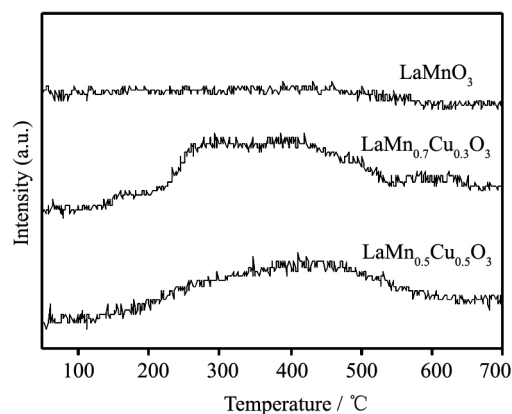


Fig. 5 H<sub>2</sub>-TPD spectra of the reduced LaMn<sub>1-x</sub>Cu<sub>x</sub>O<sub>3</sub> ( $x=0, 0.3$  and  $0.5$ )

## 2.6 H<sub>2</sub>-TPD spectra

Fig. 5 shows the TPD spectra taken on the reduced LaMn<sub>1-x</sub>Cu<sub>x</sub>O<sub>3</sub> ( $x=0, 0.3$  and  $0.5$ ) catalysts. With the increasing temperature, no desorption peak appeared for LaMnO<sub>3</sub>, while a much broader signal in the range of 200–600 °C was monitored over LaMn<sub>0.7</sub>Cu<sub>0.3</sub>O<sub>3</sub> and LaMn<sub>0.5</sub>Cu<sub>0.5</sub>O<sub>3</sub>. It could be assigned to desorption of strongly adsorbed species in the form of dissociatively adsorbed hydrogen<sup>[25]</sup>. This result suggested that H<sub>2</sub> might be adsorbed on the Cu<sup>+</sup> sites.

## 3 Conclusions

According to the catalyst characterizations, copper was assumed as an active metal for the formation of methanol, and its active oxidation state was Cu<sup>+</sup>. When less than 50% Cu was doped into LaMnO<sub>3</sub>, the perovskite structure was maintained. H<sub>2</sub> was adsorbed on Cu<sup>+</sup> sites and CO<sub>2</sub> was activated on medium CO<sub>2</sub> active species in the lattice. Then the interaction between Cu<sup>+</sup> and Mn occurred. It made a fine dispersion of active sites to adsorb much CO<sub>2</sub> and inhibited the further reduction from Cu<sup>+</sup> to Cu<sup>0</sup>, contributing to reactivity of methanol. The catalytic behavior of LaMn<sub>0.5</sub>Cu<sub>0.5</sub>O<sub>3</sub> was higher than those of LaMn<sub>0.7</sub>Cu<sub>0.3</sub>O<sub>3</sub>. This phenomenon was assigned to its stronger interaction between Cu<sup>+</sup> and Mn. However, the Cu-undoped LaMnO<sub>3</sub> had no reactivity to methanol, due to its poor adsorption of hydrogen. And the reason why LaMn<sub>0.3</sub>Cu<sub>0.7</sub>O<sub>3</sub> and LaMn<sub>0.1</sub>Cu<sub>0.9</sub>O<sub>3</sub> displayed poorer catalytic performance to methanol could be attributed to that they had no complete perovskite structure and there was no interaction between Cu and Mn to improve the reactivity.

## References:

- [1] Borodko Y, Somorjai G A. Catalytic hydrogenation of carbon oxides—a 10-year perspective. *Appl. Catal., A*, 1999, **186**: 355.
- [2] Guo X M, Mao D S, Wang S, Wu G S, Lu G Z. Combustion synthesis of CuO-ZnO-ZrO<sub>2</sub> catalysts for the hydrogenation of carbon dioxide to methanol. *Catal. Commun.*, 2009, **10**: 1661.
- [3] Jun K W, Shen W J, Rao K S R, Lee K W. Residual sodium

- effect on the catalytic activity of  $\text{Cu/ZnO/Al}_2\text{O}_3$  in methanol synthesis from  $\text{CO}_2$  hydrogenation. *Appl. Catal., A*, 1998, **174**: 231.
- [4] Zhang Y P, Fei J H, Yu Y M, Zheng X M. Energ. Methanol synthesis from  $\text{CO}_2$  hydrogenation over Cu based catalyst supported on zirconia modified  $\gamma\text{-Al}_2\text{O}_3$ . *Convers. Manage.*, 2006, **47**: 3360.
- [5] Słoczyński J, Grabowski R, Kozłowska A, Olszewski P, Stoch J, Skrzypek J, Lachowska M. Catalytic activity of the  $\text{M}/(3\text{ZnO}\cdot\text{ZrO}_2)$  system ( $\text{M}=\text{Cu, Ag, Au}$ ) in the hydrogenation of  $\text{CO}_2$  to methanol. *Appl. Catal., A*, 2004, **278**: 11.
- [6] Toyir J, Piscina P R, Fierro J L G, Homs N. Highly effective conversion of  $\text{CO}_2$  to methanol over supported and promoted copper-based catalysts: influence of support and promoter. *Appl. Catal., B*, 2001, **29**: 207.
- [7] Navarro R M, Alvarez-Galvan M C, Villoria J A, González-Jiménez I D, Rosa F, Fierro J L G. Effect of Ru on  $\text{LaCoO}_3$  perovskite-derived catalyst properties tested in oxidative reforming of diesel. *Appl. Catal., B*, 2007, **73**: 247.
- [8] Araujo G C, Lima S M, Assaf J M, Peña M A, Fierro J L G, Rangel M C. Catalytic evaluation of perovskite-type oxide  $\text{LaNi}_{1-x}\text{Ru}_x\text{O}_3$  in methane dry reforming. *Catal. Today*, 2008, **133-135**: 129.
- [9] Tien-Thao N, Alamdari H, Kaliaguine S. Characterization and reactivity of nanoscale  $\text{La}(\text{Co, Cu})\text{O}_3$  perovskite catalyst precursors for CO hydrogenation. *J. Solid State Chem.*, 2008, **181**: 2006.
- [10] Petrović S, Karanović L, Stefanov P K, Zdujić M, Terlecki-Baričević A. Catalytic combustion of methane over Pd containing perovskite type oxides. *Appl. Catal., B*, 2005, **58**: 133.
- [11] Brown Bourzutschky J A, Homs N, Bell A T. Conversion of synthesis gas over  $\text{LaMn}_{1-x}\text{Cu}_x\text{O}_{3+\delta}$  perovskites and related copper catalysts. *J. Catal.*, 1990, **124**: 52.
- [12] Nakamura T, Petzow G, Gauckler L J. Stability of the perovskite phase  $\text{LaBO}_3$  ( $\text{B}=\text{V, Cr, Mn, Fe, Co, Ni}$ ) in reducing atmosphere I. Experimental results. *Materials Research Bulletin*, 1979, **14**: 649.
- [13] Zhang R, Villanueva A, Alamdari H, Kaliaguine S. Reduction of NO by CO over nanoscale  $\text{LaCo}_{1-x}\text{Cu}_x\text{O}_3$  and  $\text{LaMn}_{1-x}\text{Cu}_x\text{O}_3$  perovskites. *J. Mol. Catal. A-Chem.*, 2006, **258**: 22.
- [14] Zhang R, Villanueva A, Alamdari H, Kaliaguine S. SCR of NO by propene over nanoscale  $\text{LaMn}_{1-x}\text{Cu}_x\text{O}_3$  perovskites. *Appl. Catal., A*, 2006, **307**: 85.
- [15] Ramaswamy V, Awati P, Tyagi A K. Lattice thermal expansion of  $\text{LaCo}_{1-x}\text{Cu}_x\text{O}_3$ . *J. Alloys Compd.*, 2004, **364**: 180.
- [16] Porta P, Rossi S, Faticanti M, Minelli G, Pettiti I, Lisi L, Turco M. Perovskite-type oxides I. structural, magnetic, and morphological properties of  $\text{LaMn}_{1-x}\text{Cu}_x\text{O}_3$  and  $\text{LaCo}_{1-x}\text{Cu}_x\text{O}_3$  solid solutions with large surface area. *J. Solid State Chem.*, 1999, **146**: 291.
- [17] Tien-Thao N, Alamdari H, Zahedi-Niaki M H, Kaliaguine S.  $\text{LaCo}_{1-x}\text{Cu}_x\text{O}_{3-\delta}$  perovskite catalysts for higher alcohol synthesis. *Appl. Catal., A*, 2006, **311**: 204.
- [18] Słoczyński J, Grabowski R, Kozłowska A, Olszewski P, Lachowska M, Skrzypek J, Stoch J. Effect of Mg and Mn oxide additions on structural and adsorptive properties of  $\text{Cu/ZnO/ZrO}_2$  catalysts for the methanol synthesis from  $\text{CO}_2$ . *Appl. Catal., A*, 2003, **249**: 129.
- [19] Toyir J, Piscina P R, Fierro J L G, Homs N. Catalytic performance for  $\text{CO}_2$  conversion to methanol of gallium-promoted copper-based catalysts: influence of metallic precursors. *Appl. Catal., B*, 2001, **34**: 255.
- [20] Fujita S I, Usui M, Takezawa N. Mechanism of the reverse water gas shift reaction over  $\text{Cu/ZnO}$  catalyst. *J. Catal.*, 1992, **134**: 220.
- [21] Jia L S, Gao J, Fang W P, Li Q B. Carbon dioxide hydrogenation to methanol over the pre-reduced  $\text{LaCr}_{0.5}\text{Cu}_{0.5}\text{O}_3$  catalyst. *Catal. Commun.*, 2009, **10**: 2000.
- [22] Peña M A, Fierro J L G. Chemical structures and performance of perovskite oxides. *Chem. Rev.*, 2001, **101**: 1981.
- [23] Minh N V, Yang I S. A raman scattering study of structural changes in  $\text{LaMn}_{1-x}\text{Co}_x\text{O}_{3+\delta}$  system. *Vib. Spectrosc.*, 2006, **42**: 353.
- [24] Minh N V, Kim S J, Yang I S. Effect of Ni on structure and raman scattering of  $\text{LaMn}_{1-x}\text{Ni}_x\text{O}_{3+\delta}$ . *Physica B*, 2003, **327**: 208.
- [25] Dong X, Zhang H B, Lin G D, Yuan Y Z, Tsai K R. Highly active CNT-promoted  $\text{Cu-ZnO-Al}_2\text{O}_3$  catalyst for methanol synthesis from  $\text{H}_2/\text{CO}/\text{CO}_2$ . *Catal. Lett.*, 2003, **85**: 237.